Progress In Electromagnetics Research B, Vol. 22, 103–119, 2010

SYNTHESIS OF SUPERCONDUCTING CIRCULAR ANTENNAS PLACED ON CIRCULAR ARRAY USING A PARTICLE SWARM OPTIMISATION AND THE FULL-WAVE METHOD

O. Barkat and A. Benghalia

Department of Electronics
University of Constantine
Algeria

Abstract—In this paper, synthesis of superconducting circular antennas mounted on circular array is designed by the combination of a method based on particle swarm and a full-wave method. Full-wave method is used for computing the resonant frequency, bandwidth, radiation pattern and the efficiency of a perfectly superconducting, or an imperfectly conducting circular microstrip, which is printed on isotropic or uniaxial anisotropic substrate. Particle Swarm Optimization (PSO) has been used to obtain the minimum side lobe level (SLL) of circular array, by varying elements excitations and/or positions. Numerical results concerning the effect of the parameters of substrate and superconducting patch on the antenna performance are presented and discussed. It is found that superconducting circular antenna could give high efficiency. Also, results show the efficiency of PSO in producing desired radiation characteristics and are in good agreement with previously published data.

1. INTRODUCTION

Microstrip antennas have a number of useful properties, which are employed as radiating or receiving elements in a wide range of microwave systems, such as radar, navigation, communication. The radiating elements in these applications can come in a variety of configurations, with the rectangular and circular patches being the most popular due to the ease of analysis and fabrication. The circular conductor printed on a dielectric substrate backed by a

Corresponding author: O. Barkat (barkatwarda@yahoo.fr).

perfectly conducting plane is used as a resonator as well as an antenna element [1]. This structure has been analyzed extensively in the last two decades, employing a wide variety of techniques, ranging from simple intuitive models to highly sophisticated techniques using the rigorous spectral domain approach with the Galerkin method.

In order to further improve the performance of patch antennas, it has been proposed to replace the conventional patch structures by superconductors. The recent successful results of high temperature superconducting thin film technology have been encouraged in the realization of microwave circuits and antennas. A major property of superconductor is very low surface resistance compared with normal metals, such as copper, silver, and gold. Using this low surface resistance Z_s, superconductors can reduce the insertion loss and obtain a rather high gain, but suffer from a very narrow bandwidth, which severely limits its application.

The radiation characteristics provided by a single element were gradually found to be inadequate. To solve this problem, an arrangement of several radiating elements called an array was developed. Uniformly excited and equally spaced antenna array has high directivity but it usually suffers from high side lobe level. To reduce the side lobe level, the array is made aperiodic by altering the positions of the antenna elements with all excitation amplitudes being non uniform. A very popular type of antenna arrays is the circular array that has several advantages, such as symmetry in azimuth, which makes them ideally suited for full 360° coverage. This advantage has been exploited for the development of broadcast antennas and direction-finding antennas. Circular antenna arrays find various applications in sonar, radar, mobile and commercial satellite communications systems [2].

During the last decade, optimizations of antenna arrays have received great attention in the problems antenna arrays. The conventional methods of linear antenna array optimization use a set of linear or nonlinear design equations and solve them to get the optimal solution. These methods are not suitable for circular array optimization. Due to the complexity of the design problem, several evolutionary approaches as genetic algorithms and particle swarm optimization (PSO) have become very popular for optimization problems in antenna arrays [3, 4].

Many authors have studied antenna array pattern synthesis by using technique PSO [3, 6], and most of these studies have only considered optimizing an array of isotropic elements and cylindrical dipoles [5, 6]. They have been given the element excitations and/or positions, allowing us to satisfy all the patterns requirements. But,

all these studies did not take the efficiency of superconducting circular antennas on uniaxial anisotropic and directivity of superconducting circular antenna mounted in circular array. For these reasons, in this paper, we use a method based on a full wave for calculating the radiation characteristics of superconducting circular antennas on uniaxial anisotropic, and PSO is used to determine a set of elements excitation coefficients and positions, which will reduce the side lobe level of the generated pattern radiation. These parameters are used in calculating the directivity of circular array of superconducting circular antennas on uniaxial anisotropic.

2. FORMULATION OF PROBLEM BY FULL-WAVE

The high T_c superconducting microstrip antenna considered in this work is shown in Figure 1. The circular patch of thickness h, with radius along the two axes x, y, respectively, is printed on a grounded uniaxial dielectric of thickness d characterized by a permittivity tensor given by.

$$\bar{\varepsilon} = \varepsilon_0 \begin{vmatrix} \varepsilon_x & 0 & 0 \\ 0 & \varepsilon_y & 0 \\ 0 & 0 & \varepsilon_z \end{vmatrix} \tag{1}$$

where $\varepsilon_x = \varepsilon_y \neq \varepsilon_z$, and the permeability will be taken as μ_0.

The formulation of dyadic Green function $\bar{G}$ of structure is based on spectral domain (SDA). In this domain, the relationship between the patch current and electric field on the circular microstrip is given by [1, 7]:

$$\tilde{E}(k_\rho) = \bar{G}(k_\rho) \cdot \tilde{K}(k_\rho) \tag{2}$$

$\tilde{K}(k_\rho)$ is the current on the microstrip, which is related to the vector Hankel transform of $K(\rho)$. The unknown currents are expanded, in

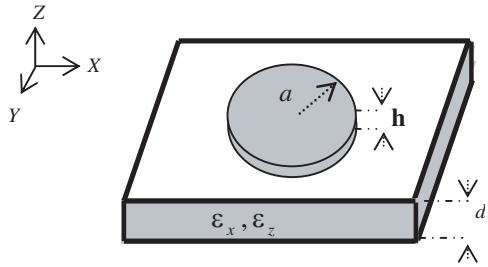

Figure 1. Cross section of the a microstrip antenna on uniaxial anisotropic media.

terms of a complete orthogonal set of basis functions, issued from the magnetic wall cavity model. It is possible to find a complete set of vector basis functions to approximate the current distribution, by noting the superposition of the currents due to TM and TE modes of a magnetic-wall cavity form a complete set. The current distribution of the nth mode of the circular microstrip can be written as [7]:

$$K_n(\rho) = \begin{cases} \sum_{p=1}^{P} a_{np}\Psi_{np}(\rho) + \sum_{q=1}^{Q} b_{nq}\Phi_{nq}(\rho) & a > \rho \\ 0 & \rho < a \end{cases} \tag{3}$$

Here a_{np} and b_{nq} are unknown coefficients. The Hankel transforms of $K_n(\rho)$ are described as [7]:

$$\tilde{K}_n(k_\rho) = \sum_{p=1}^{P} a_{np}\tilde{\Psi}_{np}(k_\rho) + \sum_{q=1}^{Q} b_{nq}\tilde{\Phi}_{nq}(k_\rho) \tag{4}$$

The basis functions $\mathbf{\Psi}_{np}$ and $\mathbf{\Phi}_{nq}$ are given by the expressions [7]:

$$\tilde{\Phi}_{nq}(k_\rho) = \beta_{nq} a J_n(\beta_{nq}a) \begin{bmatrix} \dfrac{\dot{J}_n(k_\rho a)}{\beta_{nq}^2 - k_\rho^2} & \dfrac{in}{k_\rho \beta_{nq}^2 a} J_n(k_\rho a) \end{bmatrix}^T \tag{5}$$

$$\tilde{\Psi}_{np}(k_\rho) = \begin{bmatrix} 0 & \dfrac{k_\rho a \dot{J}_n(\alpha_{np}a) J_n(k_\rho a)}{k_\rho^2 - \alpha_{np}^2} \end{bmatrix}^T \tag{6}$$

where

$$n \in N,\ p = 1:P,\ q = 1:Q$$

$J_n(\cdot)$ is the Bessel function of the first kind of order n.

In relation (2), $\bar{G}(k_\rho)$ is the spectral dyadic Green's function, which can be written as [8].

$$\bar{G} = \begin{bmatrix} G^{\mathrm{TM}} & 0 \\ 0 & G^{\mathrm{TE}} \end{bmatrix} \tag{7}$$

where

$$G^{\mathrm{TM}} = \frac{k_0}{i\omega\varepsilon_0} \frac{k_z^e \cdot \sin(k_z^e d)}{\varepsilon_x \cdot k_0 \cdot \cos(k_z^e d) + i k_z^e \cdot \sin(k_z^e d)} \tag{8}$$

$$G^{\mathrm{TE}} = \frac{k_0^2}{i\omega\varepsilon_0} \cdot \frac{\sin(k_z^h d)}{k_z^h \cos(k_z^h d) + i k_0 \sin(k_z^h d)} \tag{9}$$

k_z^e and k_z^h, the TM and TE propagation constants in the uniaxial substrate, are given by:

$$k_z^e = \left(\varepsilon_x k_0^2 - \left(\varepsilon_x k_\rho^2/\varepsilon_z\right)\right)^{1/2}, \quad k_z^h = \left(\varepsilon_x k_0^2 - k_\rho^2\right)^{\frac{1}{2}}, \quad k_0 = \omega^2 \varepsilon_0 \mu_0$$

In order to incorporate the finite thickness, the dyadic Green's function is modified by considering a complex boundary condition. The surface impedance of a high-temperature superconductors (HTSs) material, for a plane electromagnetic wave incident normally to its surface, is defined as the ratio of $|E|$ to $|H|$ on the surface of the sample. It is described by the equation [9]:

$$Z_s = \begin{cases} \sqrt{\omega\mu_0/(2\cdot\sigma)} & h \geq 3\lambda \\ 1/h\sigma & h \leq 3\lambda \end{cases} \tag{10}$$

where the conductivity $\sigma = \sigma_c$ is real for conventional conductors, and $\sigma = \sigma_n(T/T_c)^4 - i(1-(T/T_c)^4)/\omega\mu_0\lambda_0^2$ for superconductors.

The boundary condition on the surface of the circular microstrip is given by:

$$\bar{E}_{\text{scat}} + \bar{E}_{\text{inc}} - \bar{\bar{Z}}_s \cdot \bar{K}_n = 0 \tag{11}$$

Here $\bar{E}_{\text{inc}}$ and $\bar{E}_{\text{scat}}$ are tangential components of incident and scattered electric fields. Electric field is enforced to satisfy the impedance boundary condition on the circular microstrip, and the current vanishes off the circular microstrip, to give the following set of vector dual integral equations [8].

$$e_n(\rho) = \int_0^\infty dk_\rho k_\rho \bar{H}_n(k_\rho\rho) \cdot \left(\bar{\bar{G}}(k_\rho) - \bar{\bar{Z}}_S\right) \bar{K}_n(k_\rho) = 0 \quad \rho < a \tag{12}$$

$$K_n(\rho) = \int_0^\infty dk_\rho k_\rho \bar{H}_n(k_\rho\rho) \cdot \bar{K}_n(k_\rho) = 0 \quad a < \rho \tag{13}$$

where $\bar{\bar{Z}}_s = \begin{bmatrix} Z_s & 0 \\ 0 & Z_s \end{bmatrix}$

Galerkin's method is employed to solve the coupled vector integral equations of (12) and (13). Substituting the Hankel transform current expansion of (3) into (12) and (13), then, multiplying the resulting equation by $\rho\psi_{np}^+(\rho)$ ($p = 1, 2, \ldots, P$) and $\rho\phi_{nq}^+(\rho)$ ($q = 1, 2, \ldots, Q$), integrating from 0 until to a, and using Parseval's theorem for VHT, we obtain a system of $Q + P$ linear algebraic equations for each mode n, which may be written in matrix form. Following well-known procedures, we obtain the following system of linear algebraic equations:

$$\begin{bmatrix} \left(\bar{\bar{Z}}'^{\Psi\Psi}\right)_{P\times P} & \left(\bar{\bar{Z}}'^{\Psi\Phi}\right)_{P\times Q} \\ \left(\bar{\bar{Z}}'^{\Phi\Psi}\right)_{Q\times P} & \left(\bar{\bar{Z}}'^{\Phi\Phi}\right)_{Q\times Q} \end{bmatrix} \cdot \begin{bmatrix} (A')_{P\times 1} \\ (B')_{Q\times 1} \end{bmatrix} = 0 \tag{14}$$

Each element of the submatrices $\bar{Z}^{CD}$ is given by:

$$\bar{Z}'^{CD}_{ij} = \int_0^\infty dk_\rho k_\rho C^+_{ni}(k_\rho) \cdot \left(\bar{G}(k_\rho) - \bar{Z}_S\right) \cdot D_{nj}(k_\rho) \tag{15}$$

where C and D represent either ψ or φ, for every value of the integer n.

Once the impedance and resistance matrices have been calculated, the resulting system of equations is then solved, for the unknown current modes on the circular microstrip. Nontrivial solutions can exist, if the determinant of Equation (14) vanishes, that is:

$$\det\left[\bar{Z}'(f)\right] = 0 \tag{16}$$

In general, the roots of this equation are complex numbers indicating that the structure has complex resonant frequency ($f = f_r + if_i$). The bandwidth of a structure, operating around its resonant frequency, can be approximately related to its resonant frequency, though the well-known formula (BW $= 2f_i/f_r$). Once the problem is solved for the resonant frequency, the far field radiation patterns (E_θ, E_φ), for superconducting circular antenna are given.

$$\begin{bmatrix} E_\theta(\bar{r}) \\ E_\varphi(\bar{r}) \end{bmatrix} = \sum_{n=-\infty}^{+\infty} e^{in\varphi} \cdot (-i)^n \cdot e^{ikr} \cdot \bar{L}(\theta) \cdot \bar{V}(k_\rho) \cdot \left(\bar{G}(k_\rho) - \bar{Z}_S\right) \cdot \bar{K}_n(k_\rho) \tag{17}$$

where

$$\bar{V}(k_\rho) = \begin{bmatrix} 1 & 0 & -\frac{k_\rho}{k_z} \\ 0 & 1 & 0 \end{bmatrix} \text{ and } \bar{L}(\theta) = \begin{bmatrix} \cos(\theta) & 0 & -\sin(\theta) \\ 0 & 1 & 0 \end{bmatrix}$$

The electric field component is defined in the interval $0 \leq \theta \leq \pi$, $0 \leq \varphi \leq 2\pi$.

The losses in the antenna comprise dielectric loss P_d, conductor loss P_c, and radiation loss P_r are given by [10]:

$$P_r = \left(\frac{1}{4\eta_0}\right) \iint |E|^2 r^2 \sin\theta d\theta d\varphi \tag{18}$$

$$P_c = Z_s \iint |H|^2 dS \tag{19}$$

$$P_d = \left(\frac{\omega\varepsilon \mathrm{tg}\delta}{2}\right) \iint |E|^2 dV \tag{20}$$

The radiation efficiency for the lowest mode TM_{11} is given by [10]:

$$\eta = P_r/(P_r + P_c + P_d) \tag{21}$$

In order to improve the radiation characteristics of superconducting circular antennas, we mount them in array. For simplicity in analysis, the overall radiation pattern of an antenna array can be obtained by multiplying the array factor of the array and element pattern of the superconducting circular antenna. Hence, in an array of identical antennas, there are five control parameters that can be used to shape the overall pattern of the antenna array. These are the geometrical configuration of the overall array, relative displacement between the elements, excitation amplitude of the individual elements, excitation phase of the individual elements, and relative pattern of the individual elements. In this study we consider a circular array as shown in Figure 2, of N high T_c superconducting circular antennas, which are unequally spaced on the X-Y plane along a circle of radius R, and all excitation amplitudes being non uniform.

The normalized field of the array can be written as:

$$F_s(\theta, \varphi) = E_0(\theta, \varphi) \sum_{i=1}^{N} a_i e^{jk_0 R \sin(\theta) \cos(\varphi - \varphi_i))} \tag{22}$$

The Excitation coefficients (amplitude and phase) of the N elements are chosen to be: $a_i = A_i e^{j\alpha_i}$.

In a privileged direction (θ_0, φ_0), the excitation phases of the N elements are chosen to be $\alpha_i = -k_0 R \cos(\varphi_0 - \varphi_i))$.

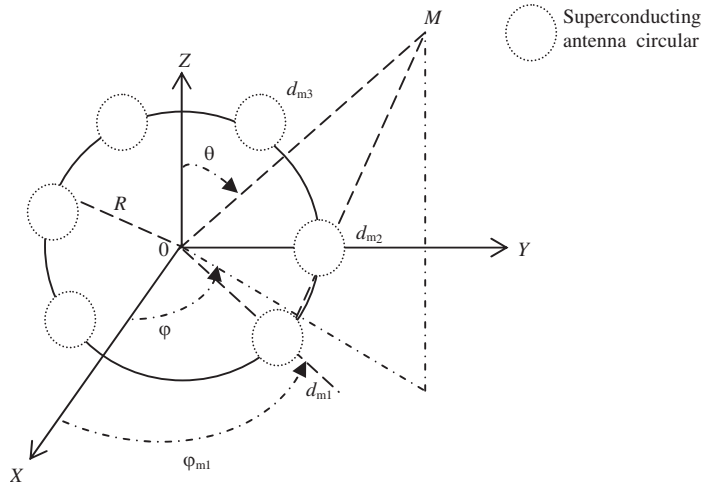

Figure 2. Geometry of a circular antenna array.

The normalized field of the array will become:

$$F_s(\theta,\varphi)=E_0(\theta,\varphi)\sum_{i=1}^{N}A_i\exp[jk_0R(\sin\theta\cdot\cos(\varphi-\varphi_i)-\sin\theta_0\cdot\cos(\varphi_0-\varphi_i))] \quad (23)$$

where

$k_0R=\sum_{i=1}^{N}d_{mi}$ and $k_0=\frac{2\pi}{\lambda}$: The wave number

$\varphi_n=\frac{2\pi}{k_0R}\sum_{i=1}^{n}d_{mi}$: Angular position of the element on the x-y plane

d_{mn}: The arc distance between the first ($i=1$) and the element n ($i=n$)

The directivity of N elements, mounted in circular array for a tilted beam in the (θ_0',φ_0') direction, can be expressed as [11]:

$$D\left(\theta_0',\varphi_0'\right)=\frac{4\pi\left|F(\theta_0',\varphi_0')\right|^2}{\int_0^{2\pi}d\varphi\int_0^{\pi}\left|F(\theta,\varphi)\right|^2\sin\theta d\theta} \quad (24)$$

$F(\theta,\varphi)$ is the field pattern of the array antenna, which is given as

$$F(\theta,\varphi)=E_0(\theta,\varphi)\sum_{i=1}^{N}A_i\exp[jk_0R(\sin\theta\cdot\cos(\varphi-\varphi_i)-\sin\theta_0\cdot\cos(\varphi_0-\varphi_i))] \quad (25)$$

where $E_0(\theta,\varphi)$ is the pattern of the single antenna, and R is the distance from the origin to the ith element.

3. PARTICLE SWARM OPTIMIZATION

PSO is a technique developed by Kennedy and Eberhart in 1995 [12]. This technique is one of the most recently developed techniques, and it is a kind of evolutionary computational technology based on the intelligent behaviour of bird flocking in searching for food. In technique PSO, the swarm is typically modeled by particles. These particles fly through hyperspace and have two essential reasoning capabilities: The memory of their own best position and knowledge of the global best. Each particle will move from its current position using the velocity and distance from current best local and global solution reached. Members of a swarm communicate good positions to each other and adjust their own position and velocity based on these good positions. So a particle has the following information to make a suitable change in its position and velocity.

The basic pseudo code for the PSO algorithm, presented below and using the global best and local bests, is:

Step 1: We have N antenna elements; the $2N$-dimensional position vector is mapped to N amplitude weights and N distance. In the beginning, a population of i-th ($i = 1, 2, \ldots, I$) particles is generated with random positions $X_i = [X_{i1}, X_{i2}, \ldots, X_{i2N}]$. Then a random velocity is assigned to each particle.

Step 2: As in all evolutionary computation techniques, there must be evaluation — Compute fitness of each particle in swarm.

Step 3: Compare the personal best (pbest) of every particle with its current fitness value. If the current fitness value is better, then assign the current fitness value to pbest and assign the current coordinates to pbest coordinates.

Step 4: Determine the current best fitness value in the whole population and its coordinates. If the current best fitness value is better than global best (gbest), then assign the current best fitness value to gbest and assign the current coordinates to gbest coordinates.

Step 5: Update using the following equations, then the new particle velocity V_i and position X_i of the $2N$ dimension of the i-th particle can be calculated by Equation (26).

$$\begin{aligned} V_i^{\text{iter}} &= W * V_i^{\text{iter}-1} + C_1 * \text{rand}_1 * \left(\text{pbest}_i^{\text{iter}-1} - X_i^{\text{iter}-1}\right) \\ &\quad + C_2 * (1 - \text{rand}_2) * \left(\text{gbest}_i^{\text{iter}-1} - X_i^{\text{iter}-1}\right) \end{aligned} \tag{26}$$

$$X_i^{\text{iter}} = X_i^{\text{iter}-1} + V_i^{\text{iter}} \tag{27}$$

Generally, W can be dynamically set with the following equation [13].

$$W = W_{\max} - \frac{W_{\max} - W_{\max}}{\text{iter}_{\max}} \cdot \text{iter} \tag{28}$$

where

$\text{iter}_{\max}$: is the maximum number of iterations.

iter: is the current number of iterations.

$W_{\max}$ and $W_{\min}$: are the upper and lower limits of the inertia weight, set to 0.5 and 0.5, respectively.

V_n: is the velocity of the particle in the $2N$ dimension, and the particle velocity is limited by a maximum value.

X_i: is the particle's coordinate in the $2N$ dimension.

pbest and gbest: are the 'personal best' and 'global best' respectively.

C_1 and C_2: are two positive constants.

Rand_1 and Rand_2: are random functions in the range $[0, 1]$.

In antenna array problems, there are many parameters that can be used to evaluate the fitness (or cost) function such as gain, side lobe level, and radiation pattern. Here, we are interested in designing a circular antenna array with minimum side lobes levels. Thus, the following fitness function is defined by:

$$\text{fitness} = \min\left(\sum_{\varphi=\varphi_0}^{\varphi=\varphi_r} \alpha \cdot (\text{NLS}(\theta,\varphi) - \text{NLSD}(\theta,\varphi)) + \sum_{i=1}^{M_s} \beta \cdot (\text{AF}_0(\theta,\varphi_i) - \text{AF}_d(\theta,\varphi_i))\right) \tag{29}$$

where $\text{NLS}(\theta,\varphi)$ and $\text{NLSD}(\theta,\varphi)$ are, respectively, the maximum sidelobe level obtained by using PSO and the desired maximum sidelobe level.

At the beginning of the optimization, the objective function was evaluated by random value of maximum sidelobe regions (φ), are: $-176^{\circ}.5$, $-149^{\circ}.7$, $-123^{\circ}.6$, $-93^{\circ}.65$, $-71^{\circ}.1$, $-40^{\circ}.76$, $40^{\circ}.05$, $69^{\circ}.7$, $94^{\circ}.15$, $133^{\circ}.1$, $158^{\circ}.35$, 180°. At the second time, a new position of maximum sidelobe regions appeared, and the function fitness could be evaluated. This procedure was repeated 20 times in our case.

$\text{AF}_0(\theta,\varphi_i)$ and $\text{AF}_d(\theta,\varphi_i)$ are the radiation patterns obtained by using PSO and the desired pattern, respectively, and M_s is the total sample points.

α and β are the weights considered to give a higher priority to minimizing the fitness function.

4. NUMERICAL RESULTS AND DISCUSSION

In order to confirm the computation accuracy, Table 1 shows the calculated resonant frequencies for the modes (TM_{11}, TM_{21}, TM_{31}, and TM_{12}). These results are compared with theoretical and experimental data, which have been suggested in [1]. We have a circular patch with a radius 7.9375 mm is printed on a substrate of thickness 1.5875 mm. Note that the agreement between our computed results and the theoretical results of [1] is very good.

The effects of temperature and thickness of a high-temperature superconducting YBCO, substrate anisotropy of antenna, on the scattering properties of circular microstrip antenna, excited in the TM_{11} are shown in Figures 3, 4.

Figure 3 shows the dependence of resonant frequency on the thickness h of superconducting patch of the antennas. It is observed that, when the film thickness h increases, the resonant frequency increases quickly until the thickness h reaches the value penetration depth λ_0. After this value, the increase in the frequency of resonance becomes less significant.

Figure 4 demonstrates relations between the real part of frequency resonance and the normalized temperature (T/T_c), where the critical temperature is used here for our data (89°). The variations of the real part of frequency is due to the uniaxial anisotropy decrease gradually with the increase in the temperature. This reduction becomes more significant for the values of temperature close to the critical temperature. These behaviours agree very well with those reported

Table 1. Comparison of resonant frequencies of the first four modes of a circular microstrip patch printed on a dielectric substrate ($a = 7.9375\,\text{mm}$, $\varepsilon_x = \varepsilon_z = 2.65$, $d = 1.5875\,\text{mm}$).

Mode	Results of Reference [1]		Our results	
	Resonant Frequency (GHz)	Quality factors (Q)	Resonant Frequency (GHz)	Quality factors (Q)
TM_{11}	6.1703	19.105	6.2101	19.001
TM_{12}	17.056	10.324	17.120	10.303
TM_{21}	10.401	19.504	10.438	19.366
TM_{01}	12.275	8.9864	12.296	8.993

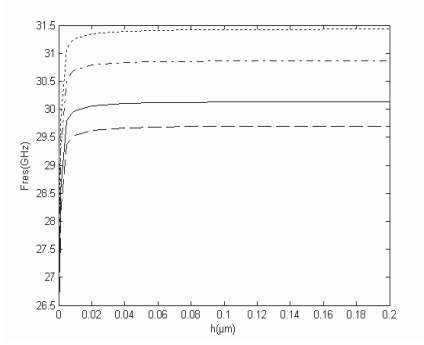

Figure 3. Real part of resonant frequency of circular microstrip antenna, Against h. ($d = 254\,\mu\text{m}$, $a = 815\,\mu\text{m}$, $T_C = 89°$, $T/T_C = 0.5$, $\lambda_0 = 1500\,\text{Å}$, $\sigma_n = 210\,\text{S/mm}$). (——) $\varepsilon_x = 9.4$, $\varepsilon_z = 11.6$; (– – –) $\varepsilon_x = 11.6$, $\varepsilon_z = 11.6$; (— · —) $\varepsilon_x = 13$, $\varepsilon_z = 10.3$; (. . . . . .) $\varepsilon_x = 10.3$, $\varepsilon_z = 10.3$.

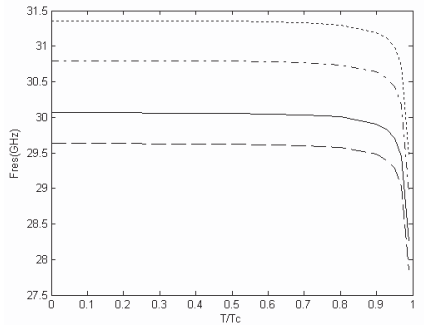

Figure 4. Real part of resonant frequency of circular microstrip antenna against T/T_C ($d = 254\,\mu\text{m}$, $a = 815\,\mu\text{m}$, $T_C = 89°$, $h = 0.02\,\mu\text{m}$, $\lambda_0 = 1500\,\text{Å}$, $\sigma_n = 210\,\text{S/mm}$). (——) $\varepsilon_x = 9.4$, $\varepsilon_z = 11.6$; (– – –) $\varepsilon_x = 11.6$, $\varepsilon_z = 11.6$; (— · —) $\varepsilon_x = 13$, $\varepsilon_z = 10.3$; (. . . . . .) $\varepsilon_x = 10.3$, $\varepsilon_z = 10.3$.

by Richard for the case of rectangular microstrip antennas [14].

Figure 5 shows the calculated radiations patterns (electric field components, E_θ; E_φ) of the superconductor circular microstrip antenna, printed on substrate thickness ($d = 254\,\mu\text{m}$), where isotropic, positive and negative uniaxial anisotropic substrates are considered. The mode excited is the TM_{11}. It is seen that the strongest radiation occurs in the broadside direction ($\theta = 0$). We also observe that the permittivity ε_z has a stronger effect on the radiation than the permittivity ε_x. The radiation pattern of an antenna becomes more directional as its ε_z increases. Another useful parameter describing the performance of an antenna is the gain. Although the gain of the antenna is related to the directivity, as illustrated in Figure 5, the gain of an antenna becomes high as its ε_z increases.

In calculation of losses, we have found that the values of the dielectric loss (P_d), conductor loss (P_c), and radiation loss (P_r) depend on frequency. We use precedents in results (electric field components, $E_theta; E_\phi$) to calculate the variation of radiation efficiency for the mode TM_{11} as a function of resonant frequency. Our results are shown in Figure 6. It is seen that the efficiency increases with decreasing frequencies. The same behaviour is found by Hansen [15].

We consider a circular array of ten isotropic elements, non-uniform spacing around a circle of radius R and non-uniform excitations of elements. In order to illustrate the capabilities of PSO to find acceptable side lobe level (SLL), equal or less than the desired value, the PSO program has been written in Matlab language, using 400 iterations. The number of particles taken is 50. The values of C_1 and C_2 are 1 and 0.95 respectively, and we have set ($W_1 = W_2 = 0.5$).

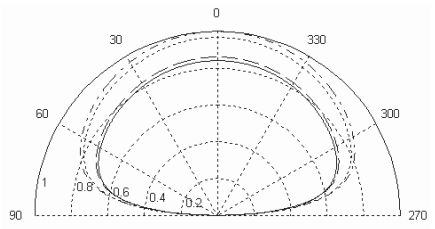

(i) φ=0 (Eθ)

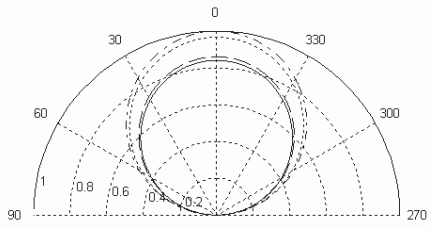

(i) φ=π/2 (Eφ)

Figure 5. Radiation pattern of circular microstrip antenna versus angle θ ($a = 815\,\mu\text{m}$, $h = 0.02\,\mu\text{m}$, $T/T_C = 0.5$, $d = 254\,\mu\text{m}$, $\lambda_0 = 1500\,\text{Å}$, $\sigma_n = 210\,\text{S/mm}$). (——) $\varepsilon_x = 9.4$, $\varepsilon_z = 11.6$; (– – –) $\varepsilon_x = 11.6$, $\varepsilon_z = 11.6$; (— · — ·) $\varepsilon_x = 13$, $\varepsilon_z = 10.3$; (. . . . . .) $\varepsilon_x = 10.3$, $\varepsilon_z = 10.3$.

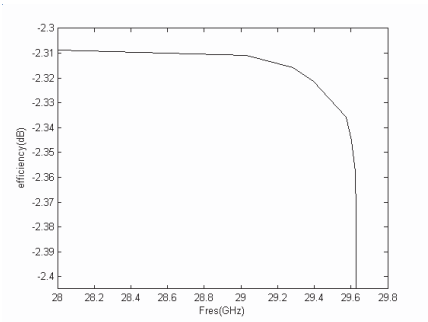

Figure 6. Circular microstrip antenna efficiency ($d = 254\,\mu$m, $a = 815\,\mu$m, $h = 0.02\,\mu$m, $T/T_C = 0.5$, $\lambda_0 = 1500\,$Å, $\sigma_n = 210\,$S/mm, $\varepsilon_x = \varepsilon_z = 11.6$, $\delta = 0.0024$).

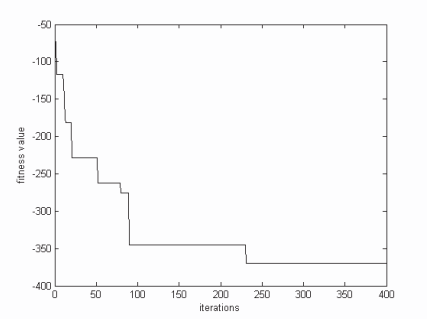

Figure 7. Convergence curve of the fitness value of the 10 element circular array versus the number of iterations.

The fitness value reaches its minimum, and this number is found to be sufficient to obtain satisfactory patterns with a desired performance. The algorithm terminates with success at global optimum point.

Figure 7 shows the convergence curves using PSO algorithm for the 10 elements placed in circular array. The program converges after 250 iterations. In general, PSO converges in a few iterations compared to other methods such as genetic algorithm (GA), since it has less complexity and can be easily implemented. The optimum parameters of amplitudes and/or positions obtained by our formulation, using PSO and formulations of [16] and [6], are shown in Table 2. These parameters can be utilized to plot the variation of radiation patterns, shown in Figure 8. Clearly, our results are generally better in terms of the sidelobe level than those suggested in [16] and [6].

The optimum parameters of amplitudes and positions obtained for 12 isotropic elements by using PSO are shown in Table 3. A comparison between results of array of N isotropic elements and N superconducting antennas is shown in Figures 9, 10. In all cases, we observe that the level of the sidelobes and level of the mainlobes of N superconducting antennas mounted in circular array are less than the level of the secondary lobes found for circular array with ten isotropic elements.

To accomplish our study, a computationally efficient technique was developed for evaluating the directivity of circular array composed of superconducting circular antennas. Figure 11 displays the calculated directivity with respect to the parameters found by PSO, for the

fundamental mode TM_{11} as a function of the beam tilt angle from the Z-axis.

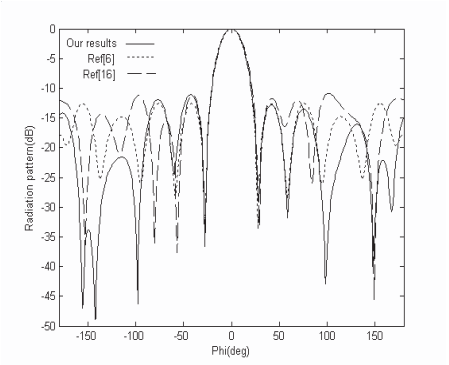

Figure 8. Radiation pattern of circular array of ten isotropic elements against φ.

Table 2. Optimized parameters of 10 isotropic elements.

n	**Our results**		**PS0 [6]**		**GA [16]**	
	I_n	d_n	I_n	d_n	I_n	d_n
1	1.0000	0.30303 λ	0.7383	0.3243 λ	0.9545	0.3641 λ
2	0.71984	0.97381 λ	0.8737	0.9747 λ	0.4283	0.4512 λ
3	0.60893	0.39089 λ	0.5782	0.4124 λ	0.3392	0.2750 λ
4	0.96059	0.92882 λ	1.000	0.9369 λ	0.9074	1.6373 λ
5	0.51031	0.40196 λ	0.7088	0.3571 λ	0.8086	0.6902 λ
6	0.92380	0.27149 λ	1.000	0.3572 λ	0.4533	0.9415 λ
7	0.89264	0.95273 λ	0.5782	0.9369 λ	0.5634	0.4657 λ
8	0.74104	0.37613 λ	0.8737	0.4124 λ	0.6015	0.2898 λ
9	0.93613	0.94104 λ	0.7383	0.9747 λ	0.7045	0.6456 λ
10	0.49359	0.30854 λ	0.7179	0.3243 λ	0.5948	0.3282 λ

Table 3. Optimized parameters of 12 isotropic elements.

n	1	2	3	4	5	6	7	8	9	10	11	12
I_n	1.00	0.543	0.652	0.843	0.986	0.765	0.343	0.873	0.546	0.459	0.789	0.988
d_n/λ	0.297	0.794	0.672	0.732	0.775	0.365	0.351	0.794	0.456	0.813	0.835	0.311

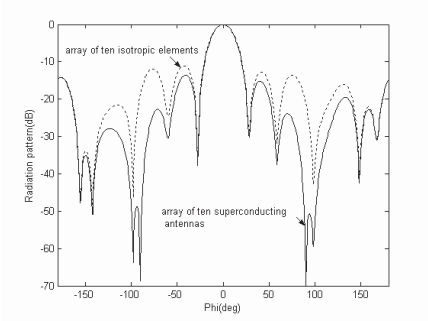

Figure 9. Radiation pattern of circular array of ten superconducting antennas, and ten isotropic elements, versus angle φ. ($d = 254\,\mu\text{m}$, $a = 815\,\mu\text{m}$, $h = 0.02\,\mu\text{m}$, $T_C = 89°$, $T/T_C = 0.5$, $\lambda_0 = 1500\,\text{Å}$, $\sigma_n = 210\,\text{S/mm}$, $\varepsilon_x = \varepsilon_z = 11.6$, $\delta = 0.0024$).

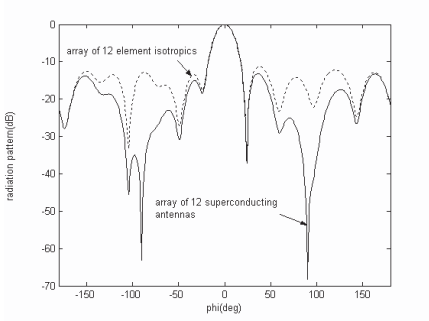

Figure 10. Radiation pattern of circular array of 12 superconducting antennas, and ten isotropic elements, versus angle φ. ($d = 254\,\mu\text{m}$, $a = 815\,\mu\text{m}$, $h = 0.02\,\mu\text{m}$, $T_C = 89°$, $T/T_C = 0.5$, $\lambda_0 = 1500\,\text{Å}$, $\sigma_n = 210\,\text{S/mm}$, $\varepsilon_x = \varepsilon_z = 11.6$, $\delta = 0.0024$).

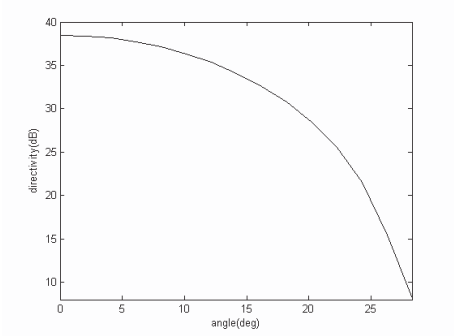

Figure 11. Calculated directivity versus beam tilt angle circular array of ten superconducting antennas ($f_r = 29.62\,\text{GHz}$, $d = 254\,\mu\text{m}$, $a = 815\,\mu\text{m}$, $h = 0.02\,\mu\text{m}$, $T_C = 89°$, $T/T_C = 0.5$, $\lambda_0 = 1500\,\text{Å}$, $\sigma_n = 210\,\text{S/mm}$, $\varepsilon_x = \varepsilon_z = 11.6$, $\delta = 0.0024$).

5. CONCLUSION

In this paper, the fullwave analysis for the superconducting circular microstrip antenna on uniaxial anisotropic media is considered. Numerical results concerning the effect of a superconductor patch, of a uniaxial substrate, and on the characteristics of the antenna are

presented. It was found that the microstrip superconducting could give high efficiency. Also we have presented an optimization technique based on PSO algorithm, which is successfully used to determine the element excitations and/or positions of non-uniform circular antenna arrays, for simultaneous reduction of the side lobe level. A comparative study, between our results and those available in the literature, shows that PSO is capable of synthesizing the unequally spaced circular arrays to produce radiation patterns with a good performance in the sidelobe region.

REFERENCES

1. Losada, V., R. R. Boix, and M. Horno, "Resonant modes of circular microstrip patches in multilayered substrates," *IEEE Transactions on Microwave Theory and Techniques*, Vol. 47, 488–497, 1999.
2. Pathad, N., G. K. Mahanti, S. K. Singh, J. K. Mishra, and A. Chakraborty, "Synthesis of thinned planar circular array antennas using modified particle swarm optimization," *Progress In Electromagnetics Research Lettres*, Vol. 12, 87–97, 2009.
3. Boeringer, D. W. and D. H. Werner, "Particle swarm optimization versus genetic algorithms for phased array synthesis," *IEEE Transactions on Antennas and Propagation*, Vol. 52, No. 3, 771–779, 2004.
4. Panduro, M. A., C. A. Brizuela, L. I. Balderas, and D. A. Acosta, "A comparison of genetic algorithm and the differential evolution method for the design of scannable circular antenna arrays," *Progress In Electromagnetics Research B*, Vol. 13, 171–186, 2009.
5. Pantoja, M. F., A. R. Bretones, F. G. Ruiz, S. G. Garcia, and R. G. Martin, "Particle swarm optimization in antenna design: Optimization of log-periodic dipole arrays," *IEEE Antennas and Propagation Magazine*, Vol. 49, No. 4, 34–47, 2007.
6. Khodier, M. and M. Al-Aqeel, "Linear and circular array optimization: A study using particle swarm intelligence," *Progress In Electromagnetics Research B*, Vol. 15, 347–373, 2009.
7. Chew, W. C. and J. A. Kong, "Resonance of non axial symmetric modes in circular micro strip disk," *J. Math. Phys.*, Vol. 21, No. 10, 2590–2598, 1980.
8. Barkat, O. and A. Benghalia, "Radiation and resonant frequency of superconducting annular ring microstrip antenna on uniaxial anisotropic media," *Springer, Journal of Infrared, Millimeter, and Terahertz Waves*, Vol. 30, No. 10, 1053–1066, 2009.

9. Cai, Z. and J. Bornemann, "Generalized spectral domain analysis for multilayered complex media and high T_c superconductor application," *IEEE Transactions on Microwave Theory and Techniques*, Vol. 40, No. 12, 2251–2257, 1992.
10. James, J. R. and P. S. Hall, *Handbook of Microstrip Antennas*, Peter Peregrinus Ltd., London, 1989.
11. Bray, M. G., D. H. Wener, D. W. Boeringer, and D. W. Machuya, "Optimization of thinned aperiodic linear phased arrays using genetic algorithms to reduce grating lobes during scanning," *IEEE Transactions on Antennas and Propagation*, Vol. 50, No. 12, 1732–1742, 2002.
12. Kennedy, J. and R. Eberhart, "Particle swarm optimization," *Proc. IEEE Int. Conf. on Neural Networks*, 1942–1948, 1995.
13. Mahmoud, K. R., M. Al-Adawy, and S. M. M. Ibrahem, "A comparison between circular and hexagonal array geometries for smart antennas systems using particle swarm optimization algorithm," *Progress In Electromagnetics Research*, Vol. 72, 75–90, 2007.
14. Richard, M. A., K. B. Bhasin, and P. C. Clapsy, "Superconducting microstrip antennas: An experimental comparison of two feeding methods," *IEEE Transactions on Antennas and Propagation*, Vol. 41, 967–974, 1993.
15. Hansen, R. C., *Electrically Small, Superdirective, and Superconducting Antennas*, John Wiley & Sons, Inc., Hoboken, New Jersey, 2006.
16. Panduro, M. A., A. L. Mendez, G. Romero, and R. F. Dominguez, "Design of non uniform circular antenna arrays for side lobe reduction using the method of genetic algorithms," *Vehicular Technology Conference VTC*, Vol. 6, 2696–2700, 2006.